

Multiband-Moments Model for the Conductivities of Chromium

J. F. Goff

U. S. Naval Ordnance Laboratory, White Oak, Silver Spring, Maryland 20910

(Received 30 March 1970)

Klemens' s moment integral formulation of the transport coefficients has been expressed in multiband form. A two-band moments model consisting of a standard and a nonstandard band has been adduced to explain the anomalies in the electrical and thermal conductivities of chromium σ and k , respectively, in the vicinity of the Néel temperature as if they were mostly the result of the changes in the band structure that occur during the antiferromagnetic transformation. It can be seen that the behavior of the Lorenz number $L = k/\sigma T$ clearly indicates that a BCS-type gap has opened over a portion of the Fermi surface during this transformation. The zero-temperature-gap ratio is $2\Delta_0 = 5.2$, a value that is in excellent agreement with the value ($2\Delta_0 = 5.1$) found experimentally by Barker *et al.* using optical reflectivity techniques. The ratio R of the antiferromagnetic and paramagnetic Fermi surfaces is 0.51, a value in very good agreement with the theoretical prediction of Asano and Yamashita. It is possible to show that a recently observed minimum in the thermal resistivity near the Néel temperature can occur even in the case of elastic scattering.

I. INTRODUCTION

The anomalies in the transport properties of the transition metals in the vicinity of chromium are caused not only by unusual scattering mechanisms, but also by their unusual band structures.¹⁻³ These band structures differ from the standard band of the theory of metals⁴ in two ways: The resulting density of states is distributed differently about the Fermi energy, and the electronic states themselves are distributed nonspherically in the Brillouin zone. Klemens' s^{5,6} formulation of the transport coefficients in terms of moment integrals of the specific conductivity $\sigma(E) \propto N(E)v^2(E)\tau(E)$, a product of the density of states, the carrier group velocity, and the relaxation time of the carrier scattering mechanisms, enables one to treat unusual distributions of states about the Fermi level; the multiband formulation of the transport coefficients⁴ considers their distribution in the Brillouin zone itself. Thus, a general formulation of these coefficients will combine these two approaches.

The Lorenz number of Cr ($L = \kappa/\sigma T$, the ratio of the thermal and electrical conductivities and the temperature) is anomalously large at all temperatures greater than 90 °K^{2,7-10}; that is, it is much greater than the expected Sommerfeld value $L_0 = 2.4453 \times 10^{-8}$ (V/deg)². While it is possible that such anomalies can be caused by resonancelike scattering mechanisms,¹¹ in pure metals at rather high temperatures it is more likely that they are due to variations in the density of states. In this case it was shown² that the anomaly could be explained by a model of the reduced specific conductivity $\sigma_r(E) = \sigma(E)/\sigma(0)$ that had many characteristics of the chromium band structure: It was symmetrical about the Fermi energy ($E = 0$), where it had a minimum and became temperature dependent below

the Néel temperature ($T_n = 312$ °K). However, the analysis used and the model developed were of single-band form; and it was not possible to describe this temperature dependence quantitatively.

In this range of temperature below T_n , a BCS-type gap opens over a part of the Fermi surface as a result of an antiferromagnetic interaction¹²; for this reason McWhan and Rice¹³ proposed that the band structure be divided dichotomously into a part A that undergoes this transformation and a part P that does not. Thus, the natural treatment of the transport coefficients of Cr is at least a two-band model. The purpose of this paper is twofold: First, Klemens' s moments formulation of the transport coefficients will be rewritten in a form more directly related to the symmetries of the band structure about the Fermi energy, and then these coefficients will be expressed in multiband form. Second, the previous² single-band model of $\sigma_r(E)$ will be decomposed into two-band form. It will be seen that the data for the Lorenz number clearly show the effect of a gap forming over a portion of the Fermi surface. The best fit of the data will give a value of the zero-temperature gap in excellent agreement with the optical gap found by Barker *et al.*¹⁴ and a ratio of the A and P surfaces in very good agreement with the theoretical calculation of Asano and Yamashita.¹⁵ Finally, the results strongly suggest that the well-known anomaly in the electrical resistivity at T_n ¹⁶ is the result of band-structure changes; scattering changes only uniformly through this temperature.

There is one cautionary remark. As of yet the lattice thermal conductivity of Cr is not known. Since this quantity will affect the measured value of L used in the present analysis, the parameters deduced herein must be regarded as approximate.

In Sec. II the moment integral formulation of the transport coefficients^{5,6} will be restated and reformulated in multiband form. In Sec. III the data will be given with the thermoelectric power corrections that were ignored previously, and the two-band model of $\sigma_r(E)$ will be developed. Finally, in Sec. IV the model will be evaluated in terms of the theoretical band structure of chromium and other transport data extant.

II. TRANSPORT COEFFICIENTS

Klemens^{5,6} showed that if the same relaxation time describes both the electrical and thermal processes and that if the phonon system is in equilibrium, the transport coefficients become

electrical conductivity:

$$\sigma = M_0, \quad (2.1a)$$

electrical thermal conductivity:

$$\kappa_e = (K/e)^2 T (M_2 - M_1^2/M_0). \quad (2.1b)$$

Lorenz number:

$$L = (K/e)^2 (M_2/M_0) - S^2, \quad (2.1c)$$

thermoelectric power:

$$S = (K/e) M_1/M_0. \quad (2.1d)$$

M_n is the n 'th moment of the specific conductivity $\sigma(\epsilon)$, where $\epsilon = E/KT$ is the reduced energy.

Klemens's formulation of these coefficients differs from other formulations^{17,18} in that he chooses $E = 0$ at the Fermi energy. Therefore,

$$M_n = - \int_{-\infty}^{+\infty} \sigma(\epsilon) \epsilon^n \frac{\partial f_0}{\partial \epsilon} d\epsilon. \quad (2.2)$$

Expand $\sigma(\epsilon)$ about the Fermi energy:

$$\sigma(\epsilon) = \sigma(0) + \sigma_1 \epsilon + \frac{1}{2} \sigma_2 \epsilon^2 + \frac{1}{6} \sigma_3 \epsilon^3 + \dots. \quad (2.3)$$

Simple metallic behavior corresponds to only the first two coefficients being non-negligible; anomalies are caused by the higher-order coefficients.¹ It is convenient to define a slightly different set of transport coefficients which will have definite symmetries in the range of the expansion (2.3). The symmetrical coefficients

$$\sigma = M_0, \quad (2.4a)$$

$$\kappa_S = (K/e)^2 T M_2, \quad (2.4b)$$

$$L_S = (K/e)^2 M_2/M_0, \quad (2.4c)$$

and the antisymmetrical coefficient

$$S\sigma = (K/e) M_1 \quad (2.4d)$$

are measurable. They differ from the coefficients (2.1) in that the retardation effect of the internal electric field on the thermal conductivity has been neglected.¹⁹ In Cr where S is large,²⁰ about 20

$\mu\text{V}/\text{deg}$ at 300 °K, this effect is only a few percent. Since these subsets of coefficients depend on the even and odd terms of the expansion (2.3) (in the range of its validity), S will tend to be independent of the conductivities. This conclusion is consistent with multiband considerations¹ and it will be seen in Sec. III that the model adduced to explain $L(\text{Cr})$ contains no thermoelectric power.

Since the relaxation time of individual scattering mechanisms is, in general, $\tau(E)^{-1} = \phi(E)T^p$, where p is some power, the reduced specific conductivity $\sigma_r(E) = \sigma(E)/\sigma(0)$ tends to be independent of the temperature dependence of the scattering processes. Thus the coefficients (2.4) can be rewritten in terms of new integrals $G_n(T)$, where

$$M_n = \sigma(0) G_n(T), \quad (2.5a)$$

$$G_n(T) = - \int_{-\infty}^{+\infty} \sigma_r(\epsilon) \epsilon^n \frac{\partial f_0}{\partial \epsilon} d\epsilon. \quad (2.5b)$$

Consequently, the transport coefficients (2.4) become the products of two factors: $\sigma(0)$, which contains implicitly the temperature dependence of the scattering mechanism and the density of states at the Fermi level, and $G_n(T)$, which gives the temperature dependence arising from anomalies in the energy dependence of $\sigma(\epsilon)$. In the range of elastic scattering, $\sigma(0)$ is the same for both conductivities; and consequently, $L = (K/e)^2 G_2/G_0$ determines this second factor for both the conductivities.

The multiband form of the moment integral formulation of the transport coefficients in Eqs. (2.1) is trivial. Since $\sigma(\epsilon) = \sum_j \sigma_j(\epsilon)$, then $M_n = \sum_j M_{jn}$. It is convenient to define the partial Lorenz numbers

$$L_A = (K/e)^2 (M_{A2}/M_{A0}), \quad L_P = (K/e)^2 (M_{P2}/M_{P0}). \quad (2.6)$$

Thus,

$$L = \sum_j (M_{j0}/M_0) L_j. \quad (2.7)$$

Since $M_{j0}/M_0 = \sigma_j/\sigma$ is a partial conductivity, Eq. (2.7) resembles a multiband form. However, it is now possible to build up the transport coefficients from a collection of nonstandard bands.

III. MODEL

The data for S^2 , where S is the absolute thermoelectric power of Cr, are shown in Fig. 1. These data are a composite of those taken from three sources: 100–330 °K, unpublished data taken by Goff² on the sample Cr(2) discussed previously; 260–340 °K, the single-crystal data of Trego and Mackintosh²⁰; and 300–1200 °K, the data of Cox and Lucke.²¹

The data taken for L are also a composite: below 330 °K they come from Goff's² sample Cr(2); above 323 °K they come from the Powell-Tye⁹ well-annealed electrolytically deposited sample. It can be seen from the ideal resistivities of these two

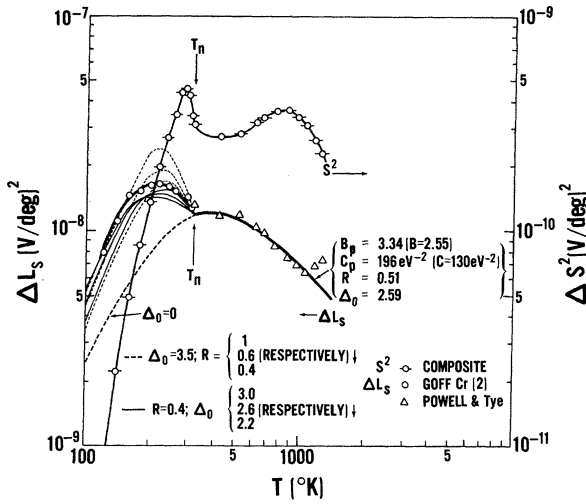


FIG. 1. Anomalous Lorenz number L of Cr and calculations for a two-band model of the Fermi surface. $\Delta L_s = (L + S^2) - L_0$, where $L_0 = 2.4453 \times 10^{-8} \text{ (V/deg)}^2$ (the Sommerfeld value) and S is the absolute thermoelectric power. The parameters are B_P , the depth of the harmonic well in the paramagnetic surface; C_P , the curvature of this well; Δ_0 , the BCS gap ratio at $T = 0^\circ\text{K}$; and R , the ratio of the antiferromagnetic and paramagnetic surfaces. $\Delta_0 = 0$ gives the model predictions for paramagnetic Cr below the Néel temperature $T_n = 312^\circ\text{K}$. B and C are the single-band values of B_P and C_P .

samples shown in Fig. 2 that they are not matched exactly at T_n . The detailed behavior of the Cr resistivities was discussed previously.²

These data were used in Eqs. (2.1c) and (2.4c) to obtain L_s : $\Delta L_s = L_s - L_0$, where the Sommerfeld value L_0 is shown in Fig. 1. Although S^2 is only about a 2% correction in L at 300°K , it affects the parameters of the model.

The significant description of these data is that $\Delta L_s > 0$ for all temperatures greater than 90°K ; initially ΔL_s varies as T^2 ; it begins to decrease at approximately $\frac{1}{2}T_n$; there is an inflection at T_n ; it then continues to decrease up to about 1000°K . The data above this highest temperature were not and are not considered. It is suggested here that they may indicate the lattice thermal conductivity, for similar ΔL have been seen in the isoelectronic^{1,22} TiFe at lower temperatures.

The single-band model of $\sigma_r(E)$ shown in Fig. 3 was proposed² to account for these characteristics in a semiquantitative way:

$$\begin{aligned} \sigma(E)/\sigma(0) &= 1 + CE^2, & |E| < \frac{1}{2}E_0 \\ \sigma(E)/\sigma(0) &= B, & |E| \geq \frac{1}{2}E_0 \end{aligned} \quad (3.1)$$

where $C = \sigma_{2E}/2\sigma(0)$ in an expansion in terms of E . The magnitude of the anomaly described above was accounted for by the constants B and C ; its tempera-

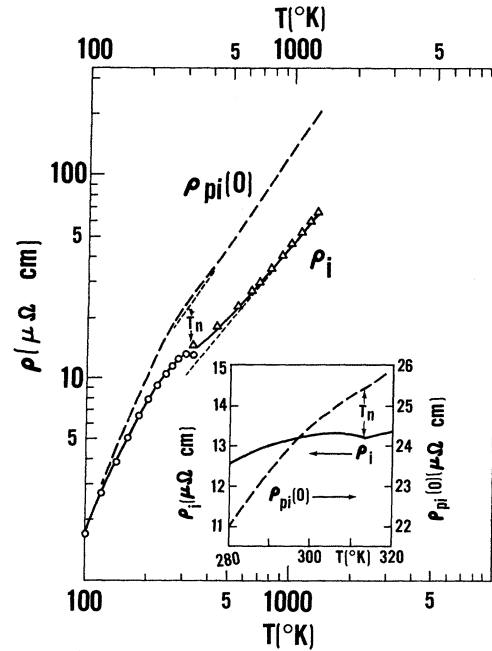


FIG. 2. Ideal electrical resistivity of Cr. Below the Néel temperature the data are those of Goff; above this temperature they are those of Powell and Tye. $\rho_{pi}(0)$ comes from the scattering factor of the transport coefficient and so contains the temperature dependence of the scattering processes.

ture dependence, by the fact that these constants were larger at temperatures less than T_n than they were above it. While this change is suggestive of a gap having been formed at lower temperatures, (such a gap would begin to disappear at $\frac{1}{2}T_n$)²³ it was not possible to account for the changes in these constants in a quantitative manner.

The values of these constants needed to fit the corrected data for ΔL_s above T_n , which is shown in Fig. 1, are $B = 2.55$ and $C = 130 \text{ eV}^{-2}$. The width of

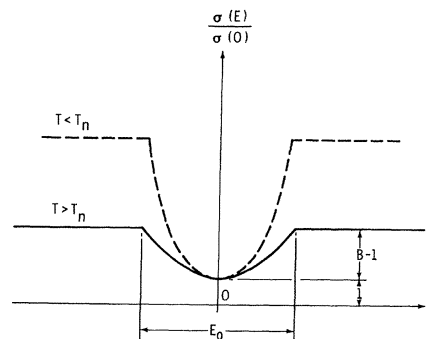


FIG. 3. Single-band model of the reduced specific conductivity $\sigma(E)/\sigma(0)$. Well curvature is $C = 4(B-1)/E_0^2$.

the well is $E_0 = 2[(B-1)/C]^{1/2} = 0.218$ eV. Since the S^2 correction increases the value of ΔL_s at the higher temperatures, the well width must be larger than the value found previously² when this correction was ignored.

The temperature dependence of ΔL_s can be treated quantitatively by dividing the Fermi surface dichotomously into a part A that undergoes an antiferromagnetic transformation below T_n and a part P that does not; such a division was suggested by McWhan and Rice.¹³ The simplest decomposition of the single-band model of Fig. 3 is shown in the top portion of Fig. 4, the paramagnetic state at $T \geq T_n$ consisting of the standard band AP and a nonstandard band with a well P . In this temperature range it makes no difference which of these two surfaces are A and P ; for if $R(E) = \sigma_{AP}(E)/\sigma_P(0)$, then

$$\sigma_r(E) = \sigma(E)/\sigma(0) = [\sigma(E)/\sigma_P(0)] \{1/[1+R(0)]\}, \quad (3.2a)$$

$$\sigma(E) = \sigma_P(0)[\sigma_P(E) + R(E)]. \quad (3.2b)$$

ΔL_s is independent of $R(0)$ as long as $\sigma(E)$ is the original surface. Thus, the solid line at $T > T_n$ in Fig. 1 and its dashed extension to lower temperatures represent the calculation of the model for either the total surface in the paramagnetic state or for $R(0) = 0$. The fact that the data for ΔL_s lie above this dashed line below T_n indicates that $R(0)$ is not zero and that the total surface has changed. It will be seen below that R has become a function of energy in this temperature range; that is, the A surface is no longer a standard band.

R is caused to be a function of energy by a BCS-

type gap opening in one of these surfaces as a result of the antiferromagnetic transformation. This gap must open in the standard band A because otherwise the low-temperature single-band model would correspond to a square well, and ΔL_s would increase much faster than T^2 . The low-temperature model is shown in the bottom portion of Fig. 4.

The P surface at all temperatures is

$$\begin{aligned} \sigma_P(E)/\sigma_P(0) &= 1 + C_P E^2, & |E| < \frac{1}{2} E_0 \\ \sigma_P(E)/\sigma_P(0) &= B_P, & |E| \geq \frac{1}{2} E_0. \end{aligned} \quad (3.3a)$$

The A surface at $T \geq T_n$ is

$$\sigma_{AP}/\sigma_P(0) = R. \quad (3.3b)$$

It is assumed that below T_n the gap opens over this surface as if only the density of states were affected:

$$\frac{\sigma_A(E)}{\sigma_P(0)} = \frac{R |E|}{(E^2 - \Delta^2)^{1/2} + \delta}, \quad |E| > \Delta \quad (3.4a)$$

$$\sigma_A(E)/\sigma_P(0) = 0, \quad |E| \leq \Delta, \quad (3.4b)$$

where $\Delta = \Delta_0 K T_n (1 - T/T_n)^{1/2}$ is the BCS gap. The anisotropy factor²⁴ δ is used here to eliminate the singularity in (3.4a); it is set small.

Since the A surface is a standard band above T_n , we have $R(E) = R$, a constant. Therefore, the constants of the new P surface are related to the old single-band constants:

$$B_P = B(1+R) - R, \quad C_P = C(1+R), \quad (3.5)$$

and the single-band model of Eqs. (3.1) can be decomposed into the two-band model of Eqs. (3.3) and (3.4) by simply adjusting Δ_0 and R to nonzero values.

A gap Δ over any conducting portion of the Fermi surface enhances ΔL_s because G_2 weights the distribution of states about the Fermi energy more heavily than does G_0 [see Eqs. (2.4c) and (2.5b)]. However, this effect is more important just below T_n than at much lower temperatures because ultimately that portion of the surface becomes insulating. The behavior of ΔL_s is quite similar to the predicted behavior of transverse acoustic attenuation in superconductors.²⁵

Representative results of calculations for different choices of Δ_0 and R are shown by the families of curves at $T < T_n$ in Fig. 1. The small dashed lines are for $\Delta_0 = 3.5$, a value chosen to be twice the BCS value in order to emphasize the effect of a large gap and several values of R . While it would be possible to fit the data at low temperatures with $R \approx 1$, the gap opens much too rapidly just below T_n ; and consequently ΔL_s is much too enhanced. On the other hand, a fit just below T_n with $R = 0.4$ leaves the A surface too insulating at the lower temperatures. It is not possible to fit the data with this value of Δ_0 . The light solid lines are for

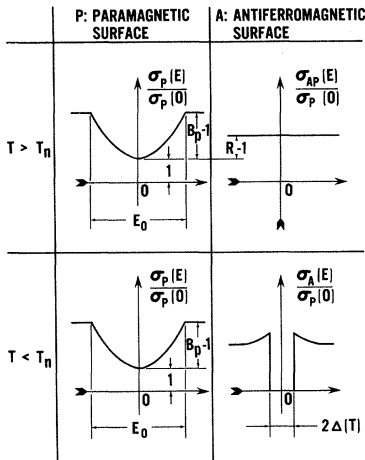


FIG. 4. Two-band model of the reduced specific conductivity consisting of a paramagnetic P and an antiferromagnetic A surface. Below the Néel temperature T_n , a BCS gap opens over the A surface.

$R = 0.4$ and several values of Δ_0 . Asano and Yamashita¹⁵ predicted that $N_{AP}/N_P = 0.41$; and indeed $R = 0.42$ gives good fit over some 40 °K at the lowest temperatures if Koehler's²⁶ experimental value $\Delta_0 = 2.2$ is used. The best fit, shown by the heavy line, is for $\Delta_0 = 2.59$ and $R = 0.51$. Even so, this fit does not agree exactly with the data just below T_n . Either the data are not precise or the model is too simple.

The components of this best-fit calculation, the partial Lorenz numbers [Eq. (2.6)] and the partial conductivities [Eq. (2.7)] are shown in Fig. 5. One sees quite clearly the gap enhancement of ΔL_A and the well enhancement of ΔL_P . The partial conductivity σ_A/σ shows the effect of carrier excitation across the gap with increasing temperature. However, the majority of the currents are carried by the P surface; the maximum contribution of the A surface is about 25% at T_n . Finally, $\sigma/\sigma_P(0)$ indicates the enhancement of the electrical conductivity as a result of the nonstandard form of the P surface. It is for this reason that the well-known^{2, 8, 13, 21, 27} concavity appears in the electrical resistivity of Cr above T_n (see Fig. 2).

This statement can be demonstrated to be at least approximately true by using Eqs. (2.4a) and (2.5a) to extract the scattering factor $\sigma_P(0)$ from the electrical conductivity. Since specific conductivities are additive, the total electrical conductivity is

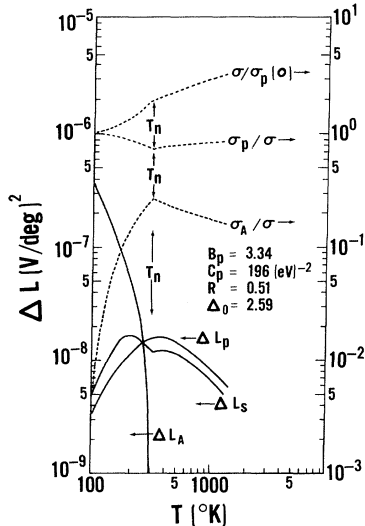


FIG. 5. Components of the two-band calculation of the transport properties of Cr for the best fit to the data. L_j is the partial Lorenz number of band j . σ_j/σ is the partial electrical conductivity of band j . ΔL_s is the composition of these components. $\sigma_P/\sigma(0)$ shows the enhancement of the electrical conductivity as a result of the nonstandard form of the P surface for this best-fit calculation.

$$\sigma = \sigma_P(0)[G_{P0}(T) + RG_{A0}(T)] = \sigma_P(0)G_0(T), \quad (3.6)$$

where $G_0(T)$ has been determined by fitting the model to ΔL_s . $\sigma_P(0)$ contains not only the temperature dependence of the scattering process but also the changes in $N(0)$. ρ_i , the ideal electrical resistivity, is shown in Fig. 2. $\rho_{pi}(0) = \rho_i G_0(T)$ is shown by the long-dashed line in the same figure. Apparently the scattering factor changes uniformly through T_n . While the concavity is not completely removed from this factor, it is suspected that this failing is a defect of the data arising from the unknown lattice thermal conductivity.

IV. CONCLUSIONS

It has been shown that the anomaly in the Lorenz number^{2, 7-10} of Cr, which appears at temperatures above 90 °K, can be explained in terms of an anomalous distribution of electronic states about the Fermi energy and throughout the Brillouin zone. A two-band model has been proposed which consists of a well-like nonstandard band for the paramagnetic P part of the Fermi surface and a standard band for the antiferromagnetic A part. Thus, the A surface somewhat resembles that used by Zittartz,^{28, 29} who calculated the effect of scattering on the electrical and thermal conductivities of the excitonic insulator. However, the P surface precludes the insulating state.

The data clearly show the effect of the BCS-type gap opening over the A surface below T_n because they are greater than the model's prediction for a completely paramagnetic surface. This result is consistent with the observation of smaller values of the Lorenz number in Mo and W (For example, it can be shown from the White-Wood data³⁰ that at 140 °K, $\Delta L/L_0$ equal for Cr, 0.61; for Mo, -0.16; for W, 0.098), although the matter is not the simple one of assuming Mo and W to be paramagnetic Cr. Since the P surface has the same form as the previous² single-band model, all qualitative justifications for that surface still apply here. The two adjustable parameters needed to fit the data below T_n are the zero-temperature-gap ratio Δ_0 and the ratio R of the A and P surfaces. The best-fit values $\Delta_0 = 2.59$ and $R = 0.51$ compare with the experimental value of Barker and co-workers,¹⁴ who found that $2\Delta_0 = 5.1$, and the theoretical ratio of the density of states $R = N_{AP}/N_P = 0.41$, which was predicted by Asano and Yamashita.¹⁵ These values are also in agreement with the McWhan-Rice¹³ results from pressure studies, although they assumed that the P surface was a standard band. It is also interesting to note that the energy of the width of the well in the P surface ($E_0 = 0.218$ eV) corresponds to an optical wavelength of about 6 μ and thus is close to the temperature-independent structure in the optical reflectivity of

Cr that was noted by Barker.¹⁴

The agreement with the prediction of Asano and Yamashita supports the contention that much of the structure of the anomalies associated with T_n comes from changes in the band structure. However, the model does not fit the data exactly at T_n ; it is somewhat low. There may be other effects.

The conductivities have been stated in a form in which they naturally factor into a term which contains the temperature dependence of the scattering processes (and the density of states at the Fermi energy) and another with the temperature dependence caused by anomalies of the density of states (and the energy dependence of the scattering processes) about the Fermi energy in the case of a single scattering process. An analysis of the Lorenz number in terms of the model determines this last factor for both the conductivities. The scattering factor is then extracted from the data by use of Eqs. (2.4a) and (2.5a). This scattering factor, which is shown in Fig. 2, suggests that the scattering processes change uniformly through the Néel temperature.

If the scattering processes are elastic, the scattering factor $\sigma_p(0)$ is the same for both the thermal and electrical conductivities. It becomes possible to compute the thermal conductivity from the more precise electrical resistivity data. From Eqs. (2.1b) and (2.4b) one finds that the thermal conductivity without the retardation effect of the internal field is

$$\kappa_s = (K/e)^2 T \sigma_p(0) G_2(T) , \quad (4.1a)$$

and the complete electrical thermal conductivity is

$$\kappa_e = \kappa_s - S^2 T \sigma_p(0) G_0(T) . \quad (4.1b)$$

In Fig. 6 are shown the ideal electrical resistivity data of Araj's¹⁶ and the ideal thermal resistivities $w = 1/\kappa$ deduced from it by the equations given above and the scattering factor shown in Fig. 2 [where it is shown as $\rho_{pi}(0) = 1/\sigma_{pi}(0)$]. One does not expect to reproduce magnitudes exactly, because the model does not quite fit the data for ΔL_s in this range of temperature; however, one does reproduce a minimum in w which has some of the characteristics of the one that was recently observed by Meaden, Rao, and Loo.¹⁰ As they pointed out, this predicted minimum occurs at a higher temperature than does the one in ρ_i , but it occurs at 325 °K rather than the observed 313.5 °K. Since this minimum seems to be related to the maximum in ΔL_p seen in Fig. 5, this difference suggests that the model does not have the A and P surfaces in correct balance.

An obvious question is whether the spin-wave system of antiferromagnetic Cr contributes a thermal conductivity that could affect the analysis. One would guess for the following reasons that it

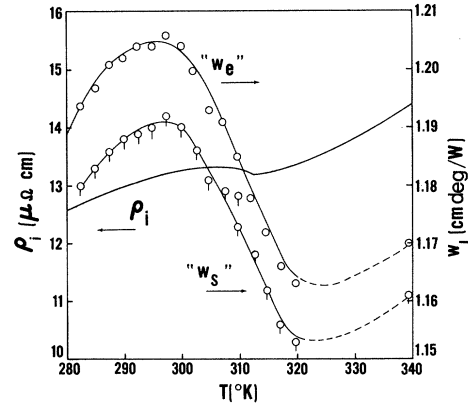


FIG. 6. Result of the calculation of the ideal thermal resistivities w_j from the data for the ideal electrical resistivity ρ_i by use of the best-fit model of the chromium Fermi surface. It was assumed that the scattering processes are completely elastic. w_e is the usual ideal thermal resistivity; w_s is this resistivity without the effect of the internal electric field.

probably does not. For a weakly interacting system of quasiparticles such as phonons or magnons, the kinetic expression of the thermal conductivity is that it is proportional to $C_v v \lambda$, the heat capacity per unit volume of the system, the group velocity, and the mean free path, respectively. Sidha and co-workers³¹ have measured in a spin-wave velocity at 300 °K of 1.29×10^7 cm/sec. Feldman³² in his recent treatment of the lattice heat capacity of Cr points out that this value is equivalent to a spin Debye temperature of about 16 000 °K. Thus, unless there is some bizarre difference in mean free paths the ratio of the magnon to the phonon conductivities is about 0.1; and the phonon conductivity has been neglected in this paper.

There are several sources of limitation and oversimplification in the model proposed:

(a) One is the assumption of a negligible lattice thermal conductivity.² While the results of the calculations imply that this assumption is approximately correct, one should expect to have to adjust the parameters of the model when this quantity is known.

(b) It has been assumed that the A surface is a standard band. This assumption greatly simplifies the calculations, is consistent with theoretical calculations, and allows for one's intuitive feeling that the A surface must differ to some extent from the P one. However, if A is to any extent nonstandard, then the relative contributions of these two surfaces will change. Even in the present model, a difference of scattering processes on the two surfaces at temperatures below T_n would cause R to vary with energy and temperature in a manner different from the BCS equation and so change the fit to the data.

In this connection one should see the work of Zittartz.^{28,29}

(c) The model contains no thermoelectric power because it is symmetric. As can be seen from Eq. (2.1d), the thermoelectric power arises from asymmetries in the specific conductivity. Since the thermoelectric power takes the same sign as the Hall coefficient,³³ it is reasonable to suppose that it is determined by asymmetries in the density of states. However, the inclusion of such asymmetries in the model to make it conform to a more realistic case would then require the density of states about the Fermi level to become a function of temperature; presumably, the reduced specific conductivity would so follow. However, the proposed model does seem to work. While this problem is beyond this paper, it does suggest that the P surface itself is further divided into symmetric and antisymmetric portions. If the antisymmetric portion were lightly populated, it would dominate the thermoelectric power,¹ but affect the conductivity little. This suggestion is essentially the same as the qualitative model that was postulated to ex-

plain the transport properties of the chromelike metals.¹

(d) The anisotropy factor δ has been set so small that its effect on the model is negligible. However, it can be shown from Eqs. (2.4c), (2.5b), and (3.4a) that if this factor is large and symmetric, it will increase the value of ΔL_A :

$$\lim_{\delta \rightarrow \infty} \Delta L_A(T_n) = (K/e)^2 F_3/F_1 - L_0 = 3.355 \times 10^{-8} \text{ (V/deg)}^2, \quad (4.2a)$$

$$F_n = - \int_0^\infty \epsilon^n \frac{\partial f_0}{\partial \epsilon} d\epsilon. \quad (4.2b)$$

Such an increase would improve the fit of the data at T_n and give a way to explain the structure in ρ_i in the immediate vicinity of T_n , which was seen by Sabine and Svenson.³⁴

ACKNOWLEDGMENT

The author would like to thank Dr. J. R. Cullen for helpful discussions about the theory of superconductivity.

¹J. F. Goff, *J. Appl. Phys.* **39**, 2208 (1968).

²J. F. Goff, *Phys. Rev. B* **1**, 1351 (1970).

³M. Shimizu, Electronic Density of States Conference, Gaithersburg, Md., 1969 (unpublished).

⁴A. H. Wilson, *The Theory of Metals* (Cambridge U. P., Cambridge, England, 1954).

⁵P. G. Klemens, Proceedings of the Fourth International Conference on Thermal Conductivity, San Francisco, 1964 (unpublished).

⁶P. G. Klemens, in *Thermal Conductivity*, edited by R. P. Tye (Academic, New York, 1969), Vol. 1, p. 1.

⁷A. F. A. Harper, W. R. G. Kemp, P. G. Klemens, R. J. Tainsh, and G. K. White, *Phil. Mag.* **2**, 577 (1957).

⁸R. W. Powell and R. P. Tye, *J. Inst. Metals* **85**, 185 (1956-57).

⁹J. P. Moore, R. K. Williams, and D. L. McElroy, Natl. Bur. Std. Special Publication No. 302 (U. S. GPO, Washington, D. C., 1968), p. 297.

¹⁰G. T. Meaden, K. V. Rao, and H. Y. Loo, *Phys. Rev. Letters* **23**, 475 (1969).

¹¹S. B. Nam and M. S. Fullenbaum, *Phys. Rev.* **186**, 506 (1969).

¹²T. M. Rice, A. S. Barker, Jr., B. I. Halperin, and D. B. McWhan, *J. Appl. Phys.* **40**, 1337 (1969).

¹³D. B. McWhan and T. M. Rice, *Phys. Rev. Letters* **19**, 846 (1967).

¹⁴A. S. Barker, Jr., B. I. Halperin, and T. M. Rice, *Phys. Rev. Letters* **20**, 384 (1968).

¹⁵S. Asano and J. Yamashita, *J. Phys. Soc. Japan* **23**, 714 (1967).

¹⁶S. Aarajs and G. R. Dunmyre, *J. Appl. Phys.* **36**, 3555 (1965).

¹⁷H. Jones, *Handbüch der Physik*, edited by S. Flügge

(Springer-Verlag, Berlin, 1956), Vol. 19, p. 227.

¹⁸J. M. Ziman, *Electronics and Phonons* (Clarendon, Oxford, England, 1960).

¹⁹J. M. Ziman, Ref. 18, p. 270.

²⁰A. L. Trego and A. R. Mackintosh, *Phys. Rev.* **166**, 495 (1968).

²¹J. E. Cox and W. H. Lucke, *J. Appl. Phys.* **38**, 3851 (1967).

²²J. F. Goff, *Bull. Am. Phys. Soc.* **12**, 348 (1967).

²³J. Bardeen and J. R. Schrieffer, in *Progress in Low Temperature Physics* (North-Holland, Amsterdam, 1961), Vol. III.

²⁴D. H. Douglass, Jr., and L. M. Falicov, in *Progress in Low Temperature Physics* (North Holland, Amsterdam, 1964), Vol. IV.

²⁵J. R. Cullen and R. A. Ferrell, *Phys. Rev.* **146**, 282 (1966).

²⁶W. C. Koehler, R. M. Moon, A. L. Trego, and A. R. Mackintosh, *Phys. Rev.* **151**, 405 (1966).

²⁷A. H. Sully, *Chromium* (Butterworths, London, 1954), p. 88.

²⁸J. Zittartz, *Phys. Rev.* **165**, 605 (1968).

²⁹J. Zittartz, *Phys. Rev.* **165**, 612 (1968).

³⁰G. K. White and S. B. Woods, *Phil. Trans. Roy. Soc. London* **251**, 273 (1959).

³¹S. K. Sidha, S. H. Liu, L. D. Muhlestein, and N. Wakabayashi, *Phys. Rev. Letters* **23**, 311 (1969).

³²J. L. Feldman, *Phys. Rev. B* **1**, 448 (1970).

³³E. B. Amitin and Yu. A. Kovalevskaya, *Fiz. Tverd. Tela* **9**, 2731 (1968) [*Soviet Phys. Solid State* **9**, 2145 (1968)].

³⁴T. M. Sabine and A. C. Svenson, *Phys. Letters* **28A**, 443 (1968).